

## *Supplementary Material*

### **Surface impacts and associated mechanisms of a moisture intrusion into the Arctic observed in mid-April 2020 during MOSAiC**

**Benjamin Kirbus\***, Sofie Tiedeck, Andrea Camplani, Jan Chylik, Susanne Crewell, Sandro Dahlke, Kerstin Ebell, Irina Gorodetskaya, Hannes Griesche, Dörthe Handorf, Ines Höschel, Melanie Lauer, Roel Neggers, Janna Rückert, Matthew D. Shupe, Gunnar Spreen, Andreas Walbröl, Manfred Wendisch, Annette Rinke

\* **Correspondence:** Benjamin Kirbus, [benjamin.kirbus@uni-leipzig.de](mailto:benjamin.kirbus@uni-leipzig.de)

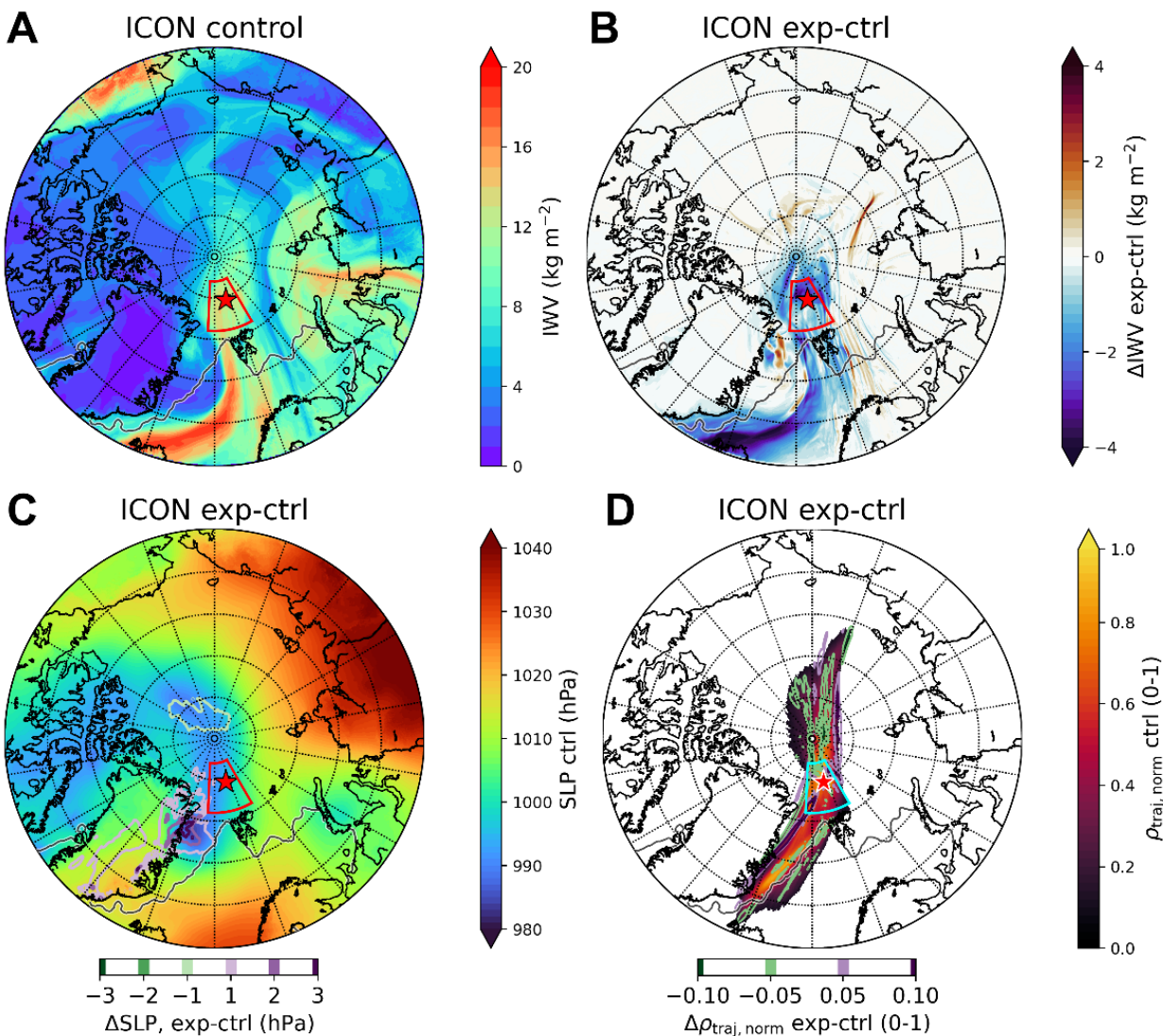
#### Table of contents

1	List of abbreviations.....	2
2	Supplementary figures.....	3

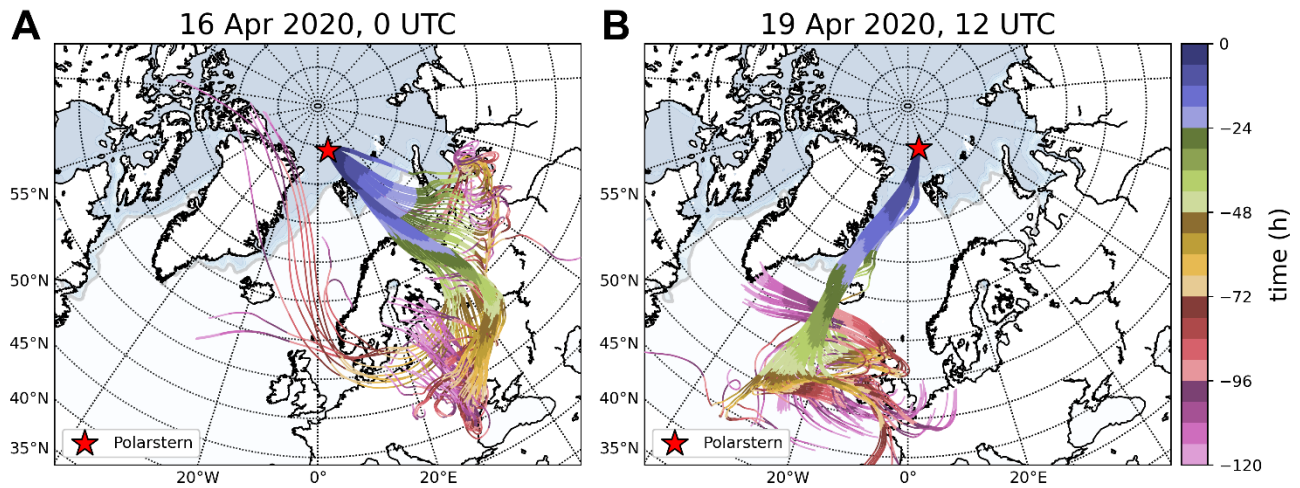
## 1 List of abbreviations

<b>Abbreviation</b>	<b>Definition</b>
ASFS	Atmospheric Surface Flux Stations
ATMS	Advanced Technology Microwave Sounder
CCN	Cloud Condensation Nuclei
CRF	Cloud Radiative Forcing
CTRL	Control Run
ECMWF	European Centre for Medium-Range Weather Forecasts
EXP	Experimental Run
HATPRO	Humidity and Temperature Profiler
ICON	Icosahedral Nonhydrostatic Model
IET	Integrated Atmospheric Horizontal Energy Transport
IVT	Integrated Water Vapor Transport
IWC	Cloud Ice Water Content
IWP	Cloud Ice Water Path
IWV	Integrated Water Vapor
KAZR	Ka-Band Zenith Radar
LAM	Limited-Area Modeling
LES	Large Eddy Simulation
LWC	Cloud Liquid Water Content
LWP	Cloud Liquid Water Path
$N_{\text{CCN}}$	CCN Concentration
$q$	Specific Humidity
SEB	Surface Energy Balance
SLALOM-CT	Snow Retrieval ALgorithm for GpM–Cross Track
SLP	Sea-Level Pressure
SSR	Surface Snowfall Rate
SSRDC	Surface Shortwave Radiation Downward, Clear Sky
SWP	Snow Water Path
$T$	Air Temperature
$T_{2\text{m}}$	2-Meter Air Temperature
$\theta_e$	Equivalent Potential Temperature
WAI	Warm Air Intrusion
WVT	Water Vapor Transport
$z$	Altitude

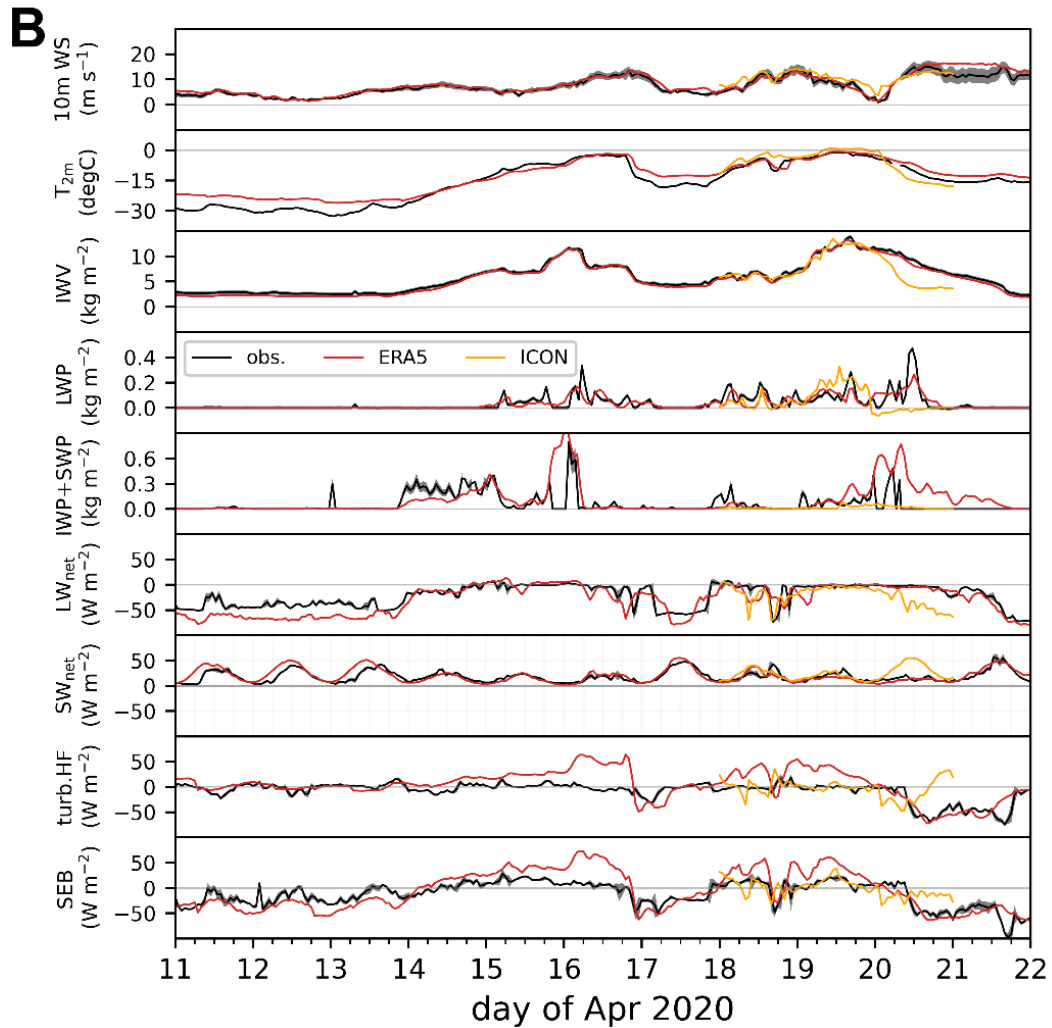
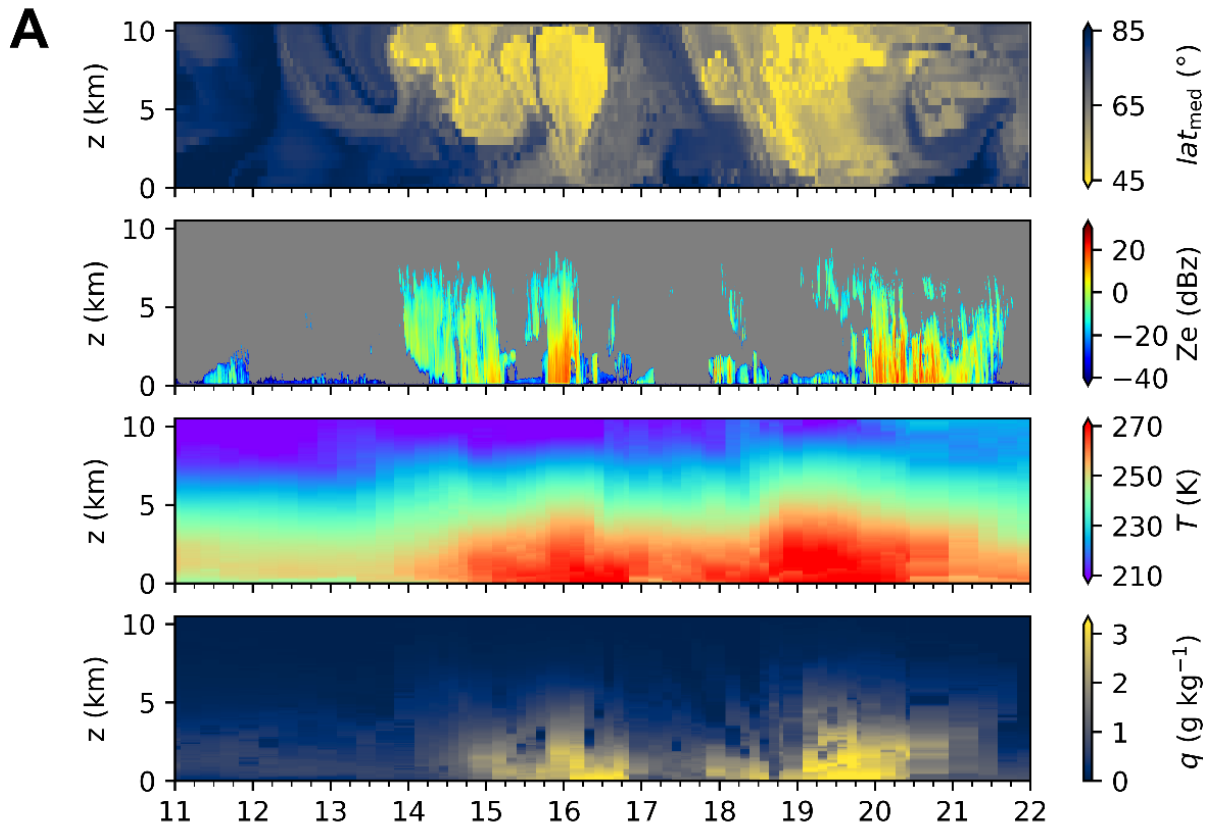
## 2 Supplementary figures



**Supplementary Figure S1:** Features of ICON-LAM simulations on 19 Apr 2020, 12 UTC, +42 h after initialization. The colored box around RV Polarstern (star symbol) indicates the starting box of the trajectory calculations. **(A)** IWV of the control run. **(B)** Difference in IWV, EXP-CTRL. **(C)** Mean SLP of CTRL (color shading) as well as SLP difference EXP-CTRL (isobars). **(D)** Normalized grid-cell density of trajectories  $\rho_{\text{traj, norm}}$  obtained after vertical and temporal integration of trajectory locations. Shown is  $\rho_{\text{traj, norm}}$  of CTRL (color shading), as well as the difference EXP-CTRL (isolines).



**Supplementary Figure S2:** 5-day backward trajectories initiated at pressure levels of 1000 hPa to 600 hPa (approx. from the surface to 5 km) in 50 hPa steps at the location of RV Polarstern. Calculations are based on LAGRANTO with ERA5 input and shown (A) for 16 April 2020, 0 UTC, (B) for 19 April, 12 UTC. The ERA5-derived sea-ice margin based on 15% ice concentration is indicated as gray line.



**Supplementary Figure S3:** Observations and model output at RV Polarstern during mid-April 2020. **(A)** Height-resolved data panels. From top to bottom: calculated median latitude of air masses during previous 5-day, observed KAZR radar reflectivity, observed radiosonde-based profiles of temperature and specific humidity (as included in Cloudnet). **(B)** Surface data panels. From top to bottom: scalar wind speed at 10 m height (10m WS),  $T_{2m}$ , IWV, LWP, combined IWP+SWP, surface radiation  $LW_{net}$  and  $SW_{net}$ , sum of turbulent sensible and latent heat fluxes (turb. HF), and total SEB. One standard deviation of measurement uncertainty is indicated by gray shading. Data sources: HATPRO (LWP, IWV), Cloudnet (IWP+SWP), Met City and ASFSs (others).